Electrochimica Acta, Vol. 35, No. 11/12, pp. 1701–1706, 1990
Printed in Great Britain.

0013–4686/90 $3.00 + 0.00

BROMIDE INDUCED ADSORPTION OF LEAD IONS ON MERCURY ELECTRODES

MARINA ZELIĆ and MILIVOJ LOVRIĆ
Zagreb Center for Marine Research, Rudjer Bošković Institute, P.O.B. 1016, 41001 Zagreb, Yugoslavia

(*Received* 17 *August* 1989; *in revised form* 27 *November* 1989)

Abstract—*Dc* polarograms of lead in $(4-x)$ M $NaClO_4 + x$ M NaBr (pH 2, $HClO_4$) may be complicated by the adsorption of neutral complex $PbBr_2$ on the surface of mercury electrode. The adsorption follows Frumkin's isotherm. If $[Br^-] = 0.117$ M, the adsorption parameters are $\Gamma_m = 1.35 \times 10^{-9}$ mol cm^{-2}, $a = 3.9$ (or $g = 3.58 \times 10^{12}$) and $\beta = 1.17 \times 10^4$ or 6.58×10^3 M^{-1} for $C^*_{Pb,tot} = 5 \times 10^{-4}$ M and 1×10^{-3} M, respectively.

Key words: metals, adsorption, anion induced.

INTRODUCTION

Complexes of metal ions with surface-active inorganic anions, or organic compounds may be strongly adsorbed on mercury electrodes[1–16]. The adsorption of lead ions from chloride[3–8, 11], bromide[3–5, 9–11, 16], iodide[3, 4, 10–16] and thiocyanate[3, 4, 11] media have been detected by a variety of techniques including double layer capacity measurements[6, 7, 14], alternating current [5, 11, 13], direct current[5, 9, 10, 12–14], radio frequency[4, 11], square-wave[11] and pulse[11] polarography, double step chronocoulometry[2, 3, 7, 15], chronopotentiometry[3, 10, 16] and chronoamperometry[8]. The *dc* polarograms of lead in the iodide medium split into a main wave and a post-wave if $3 \times 10^{-4} \leqslant [Pb(II)] \leqslant 1 \times 10^{-3}$ M and $0.01 < [I^-] \leqslant 2$ M[12–14].

Corresponding linear scan voltammograms exhibit a sharp adsorption post-peak and a broad main peak[14]. If $[Pb(II)] = 4 \times 10^{-4}$ M the main wave[12] and the main LSV peak[14] gradually develop in the concentration range of iodide between 0.01 and 0.7 M, but the further increasing of iodide concentration causes the gradual disappearance of the main wave, or peak. It has been shown that the structure of the adsorption layer of a completely covered surface does not depend on the iodide concentration inside the range between 0.015 and 1 M[14]. The splitting of the *dc* polarographic wave of lead was not observed in fluoride, chloride, bromide and thiocyanate media. However, bromide and chloride anions can induce very strong adsorption of lead if its concentration is equal, or higher than 10^{-3} M[7, 16]. The change of bromide concentration from 0.088 to 0.090 M causes the change of the lead surface concentration from 3×10^{-10} to 9×10^{-10} mol cm^{-2} if electrode potential is more positive than -0.3 V *vs sce*[16]. In 1 M chloride medium, the surface concentration of lead on mercury electrode changes from 0.5×10^{-10} mol cm^{-2} to 4×10^{-10} mol cm^{-2} if the electrode potential is changed from -0.2 to -0.1 V *vs sce* (for $[Pb(II)] = 10^{-3}$ M)[7]. If $[Pb(II)] = 2 \times 10^{-3}$ M and $[Cl^-] = 1$ M, the change of Γ_{Pb} from 1×10^{-10} to 6×10^{-10} mol cm^{-2} occurs between -0.3 and -0.25 V *vs sce*[7]. These effects have been interpreted as indicating the spontaneous formation of adsorbed crystalline bilayers of $PbBr_2$[16] or $PbCl_2$[7] on the mercury surface.

In the present communication it is shown that the *dc* polarogram of lead in bromide medium may also consist of a main wave and a post-wave if the concentration of lead is high enough. The limiting current of the main wave depends on the concentration of bromide, having the maximum when $[Br^-] = 0.15$ M. The forms of the waves indicate the adsorption of a certain $PbBr_x$ species. The *dc* polarograms of lead are simulated and compared with the experimental results. The parameters of the adsorption isotherm of lead ions in bromide medium are reported.

EXPERIMENTAL

All chemicals used, *ie* $Pb(NO_3)_2$, $NaClO_4 \cdot H_2O$, $HClO_4$ (70%) and NaBr were of analytical grade ("Merck" and "Ventron"). Deionized water obtained by Millipore Milli-Q column deionizer was used for solution perparation.

The sampled *dc* polarographic measurements were carried out by means of electrochemical analyser BAS 100A (Bionalytical Systems) and the three electrodes system consisting of an EG&G PARC model 303 static mercury drop working electrode, a platinum wire as a counter electrode and a saturated (NaCl)Ag/AgCl reference electrode. The drop time was 1 s and the scan rate 1 mV/s. Supporting electrolytes were $(4-x)$ M $NaClO_4 + x$ M NaBr + 0.01 M $HClO_4$ $(0 \leqslant x \leqslant 4)$. The solutions were previously deareated by high purity nitrogen and kept under nitrogen blanket thereafter.

THE MODEL

A *dc* polarogram of the reaction scheme:

$$\begin{array}{ccccccc} M^{2+} & \overset{+L^-}{\rightleftharpoons} & ML^+ & \overset{+L^-}{\rightleftharpoons} & ML_2 & \overset{+L^-}{\rightleftharpoons} & ML_3^- \cdots \\ \Big\Downarrow{\scriptstyle 2e^-} & & & & \Big\Downarrow{\scriptstyle \beta,\Gamma_m} & & \\ P & & & & (ML_2)_{ads}, & & \end{array} \quad \text{(I)}$$

is calculated assuming that there is a large excess of ligand, so that:

$$C_L^* = C_{L,tot}^*, \quad (1)$$

$$C_M^* = C_{M,tot}^*/(1+B), \quad (2)$$

$$C_{ML_i}^* = K_i C_{M,tot}^* (C_{L,tot}^*)^i/(1+B), \quad (3)$$

where

$$K_i = C_{ML_i}^*/(C_M^*(C_{L,tot}^*)^i),$$

$$B = \sum_{i=1}^{n} K_i (C_{L,tot}^*)^i$$

and the meanings of other symbols are defined in the Table 1. Besides, it is assumed that the redox reaction is reversible, that the product P forms an amalgam, that the complex ML_2 adsorbs at a surface of mercury electrode and that its adsorption follows Frumkin's isotherm:

$$\beta (C_{ML_2})_{x=0} \exp(a\Theta) = \Theta/(1-\Theta), \quad (4)$$

where $\Theta = \Gamma_{ML_2}/\Gamma_m$. Finally it is assumed that the stationary, planar diffusion model is applicable if the static mercury drop is used as the working electrode in the sampled *dc* polarography, so that the mass transfer can be described by the system of partial differential equations:

$$\partial C_{M,tot}/\partial t = D(\partial^2 C_{M,tot}/\partial x^2), \quad (5)$$

$$\partial C_P/\partial t = D(\partial^2 C_P/\partial x^2), \quad (6)$$

with the following initial and boundary conditions:

$$t = 0, x \geqslant 0: \; C_{M,tot} = C_{M,tot}^*, C_P = 0, \Theta = 0, \quad (a)$$

$$t \geqslant 0, x \geqslant 0: C_{L,tot} = C_{L,tot}^*, C_M = C_{M,tot}/(1+B), \quad (b)$$

$$t > 0, x \to \infty: C_{M,tot} \to C_{M,tot}^*, C_P \to 0, \quad (c)$$

$$x = 0: (C_M)_{x=0} = (C_P)_{x=0} \exp(\epsilon), \quad (d)$$

$$(C_{M,tot})_{x=0} = (1+B)(\beta b)^{-1} \times \Theta(1-\Theta)^{-1} \exp(-a\Theta), \quad (e)$$

$$D(\partial C_{M,tot}/\partial x)_{x=0} = i/nFS + \Gamma_m \, d\Theta/dt, \quad (f)$$

$$D(\partial C_P/\partial x)_{x=0} = -i/nFS,$$

where $\epsilon = nF(E - E_{1/2}^{rs})/RT$, $b = K_2 (C_{L,tot}^*)^2$ and $E_{1/2}^{rs}$ is the reversible half-wave potential of a simple redox reaction $M^{2+} + 2e^- \rightleftarrows P$. Equations (5) and (6) can be solved by the substitution $\Psi = C_{M,tot} + C_P$. The application of Laplace transforms and the modified Nicholson and Olmstead method, as described previously[20], yields a system of recursive formulae for the degree of coverage of electrode surface:

$$(\Theta_k - 1)(\Theta_k - \omega_k) - y\Theta_k \exp(-a\Theta_k) = 0, \quad (7)$$

where

$$\omega_k = (\pi dD)^{1/2} (2\Gamma_m)^{-1} C_{M,tot}^* - \sum_{i=1}^{k-1} \Theta_i (S_{k-i+1} - S_{k-1}),$$

$$y = (\pi dD)^{1/2} (2\Gamma_m \beta b)^{-1} (1 + B + \exp(-\epsilon)),$$

$$S_j = j^{1/2} - (j-1)^{1/2},$$

d is the time increment, $k = 1, 2, \ldots, M$, $M = t_d/d$ and t_d is a mercury drop life-time. Equation (7) can be solved numerically for each k. The integral equation for the *dc* polarographic current can be obtained by solving equation (6):

$$i/i_d = 2M^{1/2} \left((C_P)_{x=0,M} + \sum_{i=4}^{M-1} (C_P)_{x=0,i} (S_{M-i+1} - S_{M-i}) \right) \Big/ C_{M,tot}^*, \quad (8)$$

where $(C_P)_{x=0,k} = \Theta_k (\beta b)^{-1} (1-\Theta_k)^{-1} \exp(-\epsilon) \exp(-a\Theta_k)$, $1 \leqslant k \leqslant M$ and $i_d = nFS(D/\pi t_d)^{1/2} C_{M,tot}^*$.

Some details of mathematical procedure are given in the Appendix.

Table 1. List of symbols

$C_M, C_L, C_{ML}, C_{ML_n}$	concentrations of M^{2+}, L^-, ML, and ML_n^{2-n} respectively
$C_{M,tot}, C_{L,tot}$	total concentrations of metal and ligand ions, respectively
$C_M^*, C_L^*, C_{ML}^*, C_{ML_n}^*$	bulk concentrations of M^{2+}, L^-, ML^+ and ML_n^{2-n}, respectively
$C_{M,tot}^*, C_{L,tot}^*$	total bulk concentrations of metal and ligand ions, respectively
$(C_M)_{x=0}, C_{M,tot,x=0}$	concentrations of M^{2+} and total metal at the electrode surface
$C_P, (C_P)_{x=0}$	product concentration in the solution and at the electrode surface
D	diffusion coefficient
F	Faraday constant
i, i_d	current and limiting current of *dc* polarographic wave, respectively
i/nFS	normalized current density
K_1, K_n	stability constants of ML^+ and ML_n^{2-n} complexes, respectively, in the solution
n	number of electrons
R	gas constant
S	electrode surface area
t_d	drop life-time in *dc* polarography
V	volume of the solution
β	adsorption constant of the complex ML_2
Γ_{ML_2}	surface concentration of the adsorbed complex ML_2
Γ_m	maximum surface concentration of the complex ML_2
Θ	extent of surface coverage

RESULTS AND DISCUSSION

Sampled *dc* polarograms were recorded at a constant ionic strength ($[NaClO_4] + [NaBr] = 4$ M) and acidity (pH 2). Four series of measurements were performed in which the total concentration of lead ions was kept at 5×10^{-5}, 1×10^{-4}, 5×10^{-4} and 1×10^{-3} M. If the metal content was higher, precipitation of $PbBr_2$ occurred. When $[Pb]_{tot} = 0.0025$ M the solid phase appeared if $[B] \geq 0.117$ M. The solubility product calculated from this experimental result ($\log K_s = -5.63$) was in very good agreement with the literature[17] value of -5.68. For this calculation, the distribution of all complex species in the solution, based upon the recommended values of their formation constants ($\log K_1 = 1.48$, $\log K_2 = 2.5$, $\log K_3 = 3.5$, $\log K_4 = 3.5$, $\log K_5 = 2.7$)[17], was taken into consideration.

If the total metal concentration is 10^{-4} M, or lower, only one wave, corresponding to a reversible two-electron diffusion controlled process, appears irrespective of the bromide level. However, if the lead concentration is raised to 5×10^{-4} M, two waves are gradually formed by successive additions of bromide ions (Fig. 1A). The first one never makes more than 42% of the total current while the second becomes steeper as separation of the two waves is more pronounced. A single, but very steep wave appears in 0.032 M Br^- (the third curve from the left in Fig. 1A). The first sign of the separation of waves can be noticed in 0.047 M Br^- while in 0.063 M Br^- the waves are already well separated (curves 4 and 5 from the left, Fig. 1A). Maximum separation occurs between 0.1 and 0.2 M Br^-. After that the first wave starts to diminish if the ligand concentration is further increased, while the second one looses its steepness. Finally, when $[Br^-] > 1$ M, only one wave is obtained with the same slope as observed in the pure perchlorate medium. If $[Pb]_{tot} = 0.001$ M the first wave can make up to 80% of the total current (Fig. 1B). Two waves are separated by a small minimum. The second wave is very steep and exhibits a pronounced maximum. If a ligand concentration is constant, the limiting current of the first wave depends linearly on the concentration of lead ions between 5×10^{-4} and 2.5×10^{-3} M, but the second wave is independent of it. These waves are obviously a main wave and a post-wave caused by the adsorption of a certain complex $PbBr_x^{2-x}$ species existing in the limiting range of bromide concentrations. The slope of the post-wave and the minimum separating the two waves indicate the influence of strong lateral attractions between the adsorbed species[18–20]. The maximum on the post-wave probably belongs to the class of maxima of the third kind[21].

Using the recommended values of the stability constants[17] the distribution diagram of dissolved $PbBr_x^{2-x}$ complexes is obtained and presented in Fig. 2. When the heights of the first *dc* wave (solid dots) are plotted against the logarithms of bromide concentrations, striking similarity with the percentage of $PbBr_2$ in the solution becomes evident. Many other adsorption dependent results, such as peak heights in the square-wave voltammetry and differential pulse polarography, are connected with concentration of $PbBr_2$ in the same way. This is the

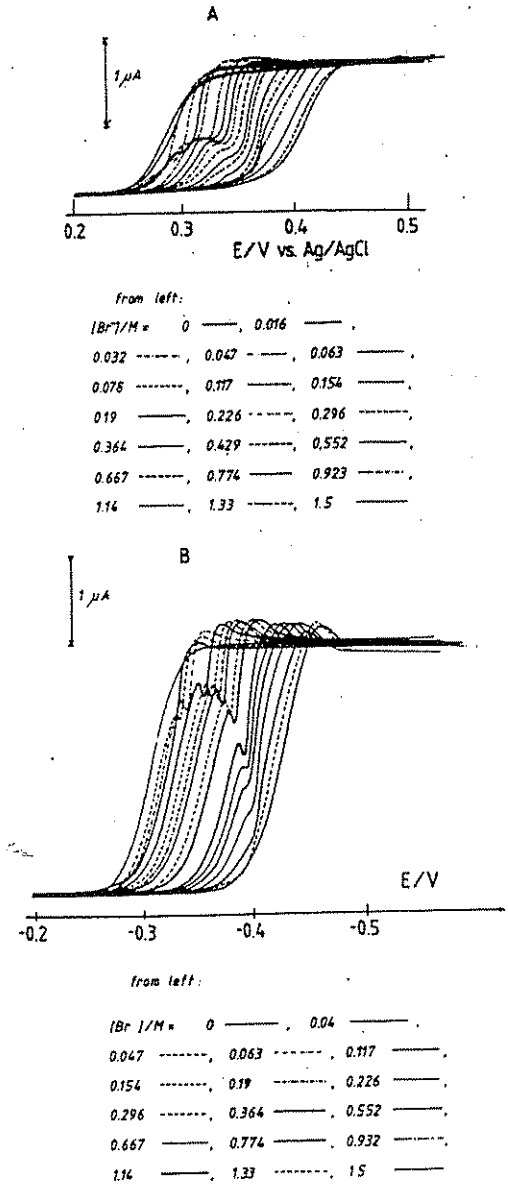

Fig. 1. Sampled *dc* polarograms of 5×10^{-4} mol dm^{-3} (A) and 1×10^{-3} mol dm^{-3} (B) solutions of Pb(II) in the system $(4 - x)$ mol dm^{-3} $NaClO_4 + x$ mol dm^{-3} Br^-, pH 2 ($HClO_4$). Concentrations of Br^- are given in the legend. SMDE; $t_d = 1$ s; $\Delta E = 1$ mV s^{-1}.

indication that the neutral complex $PbBr_2$ adsorbs on the mercurcy electrode surface modified by the adsorbed bromide ions. Assuming that the adsorption of $PbBr_2$ follows Frumkin's isotherm we have tried to determine the parameters of the adsorption isotherm by the simulation of *dc* polarograms using equations (7) and (8).

The faradaic response depends on three independent parameters: Γ_m, β and a. It was assumed that the maximum surface concentration of the adsorbed complex Γ_m does not change significantly in the potential range inside which the *dc* polarogram develops. Using recommended stability constants[17], $t_d = 1$ s, $T = 298$ K and $D = 8.5 \times 10^{-6}$ cm^2 s^{-1}[16],

Γ = coverage
β = exp function of coverg
a = ~~a~~ fractional coverage

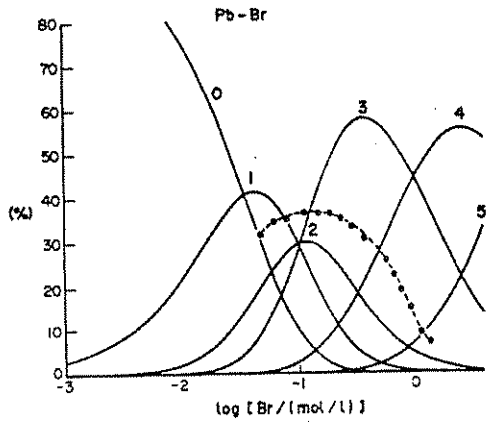

Fig. 2. Theoretical distribution of relative concentrations $PbBr_i^{2-x} C^*_{m,tot}$ of $PbBr_i^{2-x}$ complex species in the solution: (0) Pb^{2+}, (1) $PbBr^+$, (2) $PbBr_2$, (3) $PbBr_3^-$, (4) $PbBr_4^{2-}$ and (5) $PbBr_5^{3-}$; $C^*_{Pb,tot} = 0.001$ mol dm^{-3}; $I = 4$ mol dm^{-3}; $\log K_1 = 1.48$, $\log K_2 = 2.5$, $\log K_3 = 3.5$, $\log K_4 = 3.5$ and $\log K_5 = 2.7$[24]. Broken line: relative heights of the *dc* main waves from the Fig. 1B.

these three parameters were changed until satisfactory agreement with experiments was achieved. The *dc* polarograms are very sensitive to the change of adsorption parameters, which enables their precise determination if the applied model is correct. The results are shown in the Fig. 3. For $[Br^-] = 0.117$ M the parameters are $\Gamma_m = 1.35 \times 10^{-9}$ mol cm^{-2}, $a = 3.9$ (or $g = 3.58 \times 10^{12}$) and $\beta = 1.17 \times 10^4$ M^{-1} (for $C^*_{Pb,tot} \leqslant 5 \times 10^{-4}$ M), or $\beta = 6.58 \times 10^3$ M^{-1} (for $C^*_{Pb,tot} = 1 \times 10^{-3}$ M). The maximum surface concentration Γ_m is somewhat higher than the geometrically estimated limiting monolayer concentration of bromide ions (1.1×10^{-9} mol cm^{-2}[3, 16]). This may indicate that a more complex surface structure, consisting partly of two layers of $PbBr_2$ molecules, is formed. We were not able to fit in all experimental results with the single value of the surface stability constant β. The simultations indicate that β decreases as $C^*_{Pb,tot}$ increases. This could be ascribed to the attractions inside the layer if we assume that in the ordered structure the complex ions support each other, while their bonds with the mercury surface covered by initially adsorbed bromide ions become weaker. However, it is hard to say anything about the structure of the adsorbed layer solely on the basis of *dc* polarographic measurements[22].

The dependence of theoretical *dc* polarograms on total bulk concentrations of lead and bromide ions are shown in Figs 4 and 5. The form of the wave depends on the concentration of $PbBr_2$ in the solution, which itself is a function of $C^*_{Pb,tot}$ and $C^*_{Br,tot}$. Logarithmic analyses of some characteristic waves are displayed in the Fig. 4B. If lead concentration is very low (curve 1, Fig. 4A), a single wave appears. The slope of a lower part of its logarithmic analysis is equal to 29 mV/d.u. (curve 1, Fig. 4B), but the slope of the upper part is higher (23 mV/d.u.). Its half-wave potential is shifted for -8 mV from the reversible $E_{1/2}$. It is a post-wave. If the lead concentration is increased (curve 2), the lower part of the wave and its half-wave potential are shifted in the negative direction, but the uppermost part is not

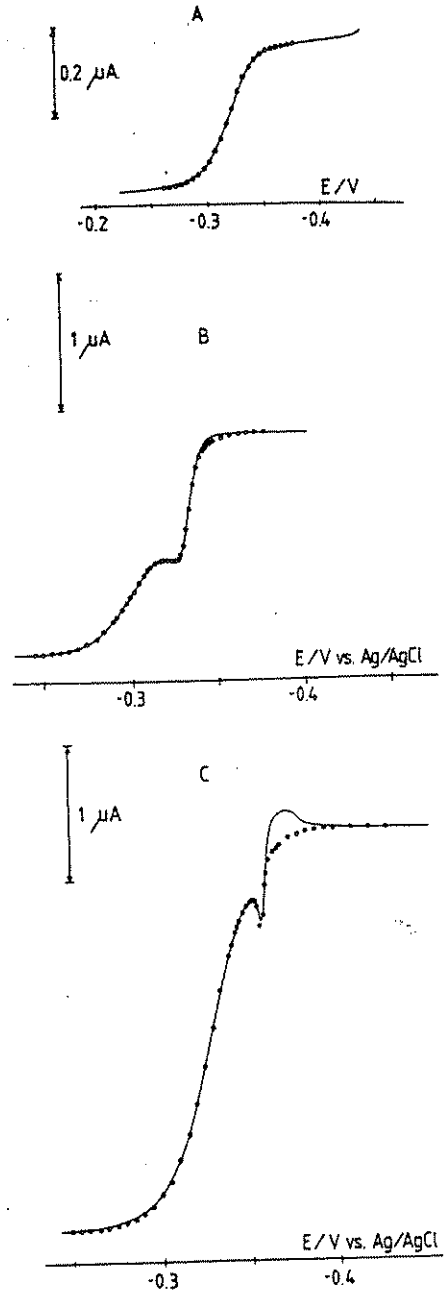

Fig. 3. The comparison between the experimental (full line) and the theoretical (points) *dc* polarograms of 1×10^{-4} dm^{-3} (A), 5×10^{-4} (B) and 1×10^{-3} mol dm^{-3} (C) lead in 0.117 mol dm^{-3} Br^- ($I = 4$ mol dm^{-3} $NaClO_4$; experimental parameters as in the Fig. 1). Only $(PbBr_2)_{ads}$ assumed, $\log \beta = 4.07$ (A, B) and 3.82 (C); $t_d = 1$ s; $D = 8.5 \times 10^{-6}$ cm^2 s^{-1}; $a = 3.9$; $\Gamma_m = 1.35 \times 10^{-9}$ mol cm^{-2}. Stability constants of dissolved complexes as in the Fig. 2.

shifted proportionally and the wave becomes steeper. Its logarithmic analysis possesses two asymptotes (29 mV/d.u. and 23 mV/d.u.) with a steep middle part. It is a post-wave influenced by the attractions in the adsorbed layer. The main wave develops in the range $300 \leqslant (C^*_{Pb,tot}/\Gamma_m)/\text{cm}^{-1} \leqslant 1500$ (curves 3–5). It may be separated from the postwave by very

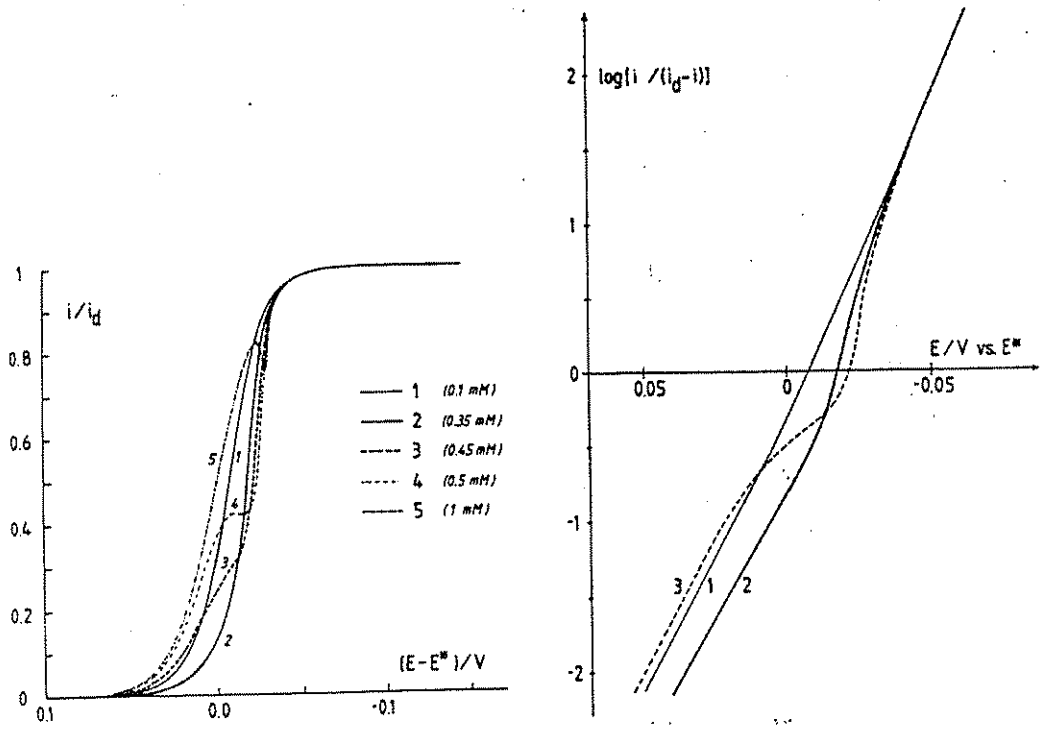

Fig. 4. (A) The dependence of the theoretical *dc* polarograms of lead in 0.117 mol dm^{-3} Br^- on the total bulk concentration of lead ions. $C^*_{Pb,tot} = 1 \times 10^{-4}$ (1), 3.5×10^{-4} (2), 4.5×10^{-4} (3) 5×10^{-4} (4) and 1×10^{-3} mol dm^{-3} (5). All parameters as in the Fig. 3. (B) Logarithmic analyses of the waves from the Fig. 4A. $C^*_{Pb,tot} = 1 \times 10^{-4}$ (1), 3.5×10^{-4} (2) and 4.5×10^{-4} mol dm^{-3} (3).

narrow depression. The post-waves are very steep. Theoretical *dc* polarograms shown in Fig. 5 were calculated assuming that the structure of the adsorbed layer on completely covered mercury surface does not depend on bromide concentration in the solution. This hypothesis was made on the basis of experimentally determined properties of the adsorbed PbI_2 layer on mercury surface[14]. The gradual development and the diminishment of the main wave can be noticed.

The similarity of Figs 1 and 5 confirms the hypothesis that the observed changes of polarographic response may be ascribed to the adsorption of $PbBr_2$ complex. Some differences in detail, however, show that the model cannot describe the fine structure of the adsorption process. These differences may be caused by neglecting the weak adsorption of all other complexes.

Presented results agree with previously described phenomena observed in chloride[7] iodide[12–14, 16]

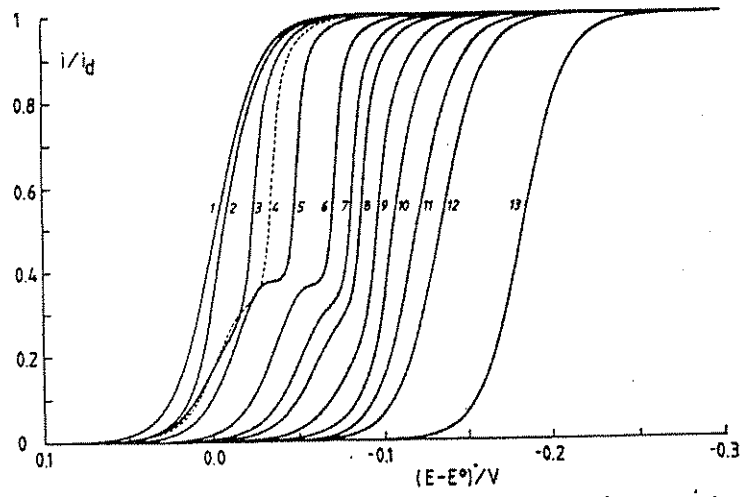

Fig. 5. The dependence of the theoretical *dc* polarograms of 5×10^{-4} mol dm^{-3} Pb(II) on the total bulk concentration of Br^- ions. $C^*_{Br,tot} = 0.008$ (1), 0.016 (2), 0.032 (3), 0.047 (4), 0.078 (5), 0.190 (6), 0.296 (7), 0.364 (8), 0.552 (9), 0.774 (10), 1.14 (11), 1.50 (12) and 4.0 mol dm^{-3} (13). All parameters as in Fig. 4.

and bromide[16] media. In each medium the condensed structure of the corresponding PbX_2 molecules appears at the surface of mercury electrode. It seems that the nature of a certain structure depends on the electrode potential. If the potential is more positive than -0.2 V *vs sce*, the structure can be described as a two-dimensional precipitate[7, 16]. *dc* polarographic waves of lead develop between 0.25–0.45 V *vs sce*, depending on the ligand concentration. In this potential range the formation of the surface structure of PbI_2[12–14], or $PbBr_2$ can be better described as the adsorption which follows Frumkin's isotherm.

Acknowledgements—This study is a contribution to the joint project of the Institute of Applied Physical Chemistry, Nuclear Research Center, Jülich and Center for Marine Research Zagreb, "Rudjer Boskovic" Institute Zagreb. Financial support by the International Bureau of KFA, Jülich, within the frame of the bilateral research agreement between S.F.R. Yugoslavia and F.R.G. is gratefully acknowledged.

In addition it was partially supported by the U.S. National Science Foundation and Self-Management Council for Scientific Research of S.R. Croatia through funds made available from the U.S.–Yugoslav Joint Board on Scientific and Technical Cooperation under the project JFP Nr 679.

REFERENCES

1. F. C. Anson, *Acc. Chem. Res.* **8**, 400 (1975).
2. D. J. Barclay and F. C. Anson, *J. electroanal. Chem.* **28**, 71 (1970).
3. R. W. Murray and D. J. Gross, *Anal. Chem.* **38**, 392 (1966).
4. G. C. Barker, in *Transactions of the Symposium on Electrode Processes* (Edited by E. Yaeger), p. 325, Wiley, New York (1961).
5. A. M. Bond and G. Hefter, *J. electroanal. Chem.* **31**, 477 (1971); **42**, 1 (1973); **68**, 203 (1976).
6. B. Timmer, M. Sluyters-Rehbach and J. H. Sluyters, *J. electroanal. Chem.* **18**, 93 (1968).
7. M. Sluyters-Rehbach, J. S. M. C. Breukel, K. A. Gijsbertsen, C. A. Wijnhorst and J. H. Sluyters, *J. electroanal. Chem.* **38**, 17 (1972).
8. M. Caselli and P. Papoff, *J. electroanal. Chem.* **23**, 41 (1969).
9. M. C. Montemayor and E. Fatas, *J. electroanal. Chem.* **246**, 271 (1988).
10. D. J. Gross and R. W. Murray, *Anal. Chem.* **38**, 405 (1966).
11. G. C. Barker and J. A. Bolzan, *Fresenius Z. anal. Chem.* **216**, 215 (1966).
12. V. Klemenčić and I. Filipović, *Croat. Chem. Acta* **31**, 29 (1959).
13. V. S. Srinavasan and A. K. Sundaram, *Aust. J. Chem.* **15**, 729, 734 (1962).
14. I. Filipović, M. Tkalčec, B. Mayer and I. Piljac, *Croat. Chem. Acta* **41**, 145 (1969).
15. V. F. Vargalyuk and Yu. M. Loshkharev, *Elektrokhimiya* **14**, 1421 (1978); *Ukrain. Khim. Zh.* **47**, 22 (1981).
16. H. B. Herman, R. L. McNeely, P. Surana, C. M. Elliott and R. W. Murray, *Anal. Chem.* **46**, 1258 (1974).
17. R. M. Smith and A. E. Martell, *Critical Stability Constants, Vol. 4: Inorganic Complexes*. Plenum Press, New York (1976).
18. E. Laviron in *Electroanalytical Chemistry*, Vol. 12 (Edited by A. J. Bard) p. 53. Marcel Dekker, New York (1983).
19. E. Laviron, *J. electroanal. Chem.* **52**, 395 (1974); **62**, 245 (1975); **105**, 25 (1979).
20. M. Lovrić, *J. electroanal. Chem.* **175**, 33 (1984).
21. A. N. Frumkin, N. V. Fedorovich, B. B. Damaskin, E. V. Stenina and V. S. Krylov, *J. electroanal. Chem.* **50**, 103 (1974).
22. A. Sadkovski, *J. electroanal. Chem.* **97**, 283 (1979); 105, 1 (1979).

APPENDIX: THE DEVELOPMENT OF EQUATIONS (7) AND (8)

If the variable $\Psi = C_{M,tot} + C_p$ is introduced, equations (5) and (6) transform to a partial differential equation:

$$\partial\Psi/\partial t = D(\partial^2\Psi/\partial x^2), \tag{A1}$$

with initial and boundary conditions:

$$t = 0;\ x \geqslant 0:\ \Psi = C^*_{M,tot}, \tag{g}$$

$$t > 0;\ x \to \infty:\ \Psi \to C^*_{M,tot}, \tag{h}$$

$$x = 0:\ D(\partial\Psi/\partial x)_{x=0} = \Gamma_m\, d\Theta/dt, \tag{i}$$

$$\Psi_{x=0} = (\beta b)^{-1}(1 + B + \exp(-\varepsilon))\Theta(1-\Theta)^{-1} \times \exp(-a\Theta). \tag{j}$$

Equation (A1) can be solved by Laplace transformations. Notice that $\mathcal{L}(d\Theta/dt) = s\mathcal{L}\Theta$ (because $\Theta = 0$ if $t = 0$) and that:

$$\mathcal{L}^{-1}(s^{1/2}\mathcal{L}\Theta) = \mathcal{L}^{-1}(s\mathcal{L}\Theta/s^{1/2}) = \pi^{-1/2}(\partial/\partial t)\int_0^t \Theta(t-\tau)^{-1/2}\,d\tau.$$

The solution of equation (A1) reads:

$$\Psi_{x=0} = C^*_{M,tot} - \Gamma_m(\pi D)^{-1/2}(\partial/\partial t)\int_0^t \Theta(t-\tau)^{-1/2}\,d\tau. \tag{A2}$$

By the method of numerical integration[20], it can be transformed to:

$$\Psi_{k,x=0} = C^*_{M,tot} - 2\Gamma_m(\pi dD)^{-1/2} \times \left[\Theta_k + \sum_{i=1}^{k-1}\Theta_i(S_{k-i+1} - S_{k-1})\right]. \tag{A3}$$

Equation 7 is obtained by the introducing of equation (A3) into condition (j).

The solution of equation (6) in Laplace space reads $\mathcal{L}(C_p)_{x=0} = (sD)^{-1/2}\mathcal{L}(i/nFS)$ whence $\mathcal{L}(i/nFS) = D^{1/2}\, s\,\mathcal{L}(C_p)_{x=0}/s^{1/2}$ and:

$$i/nFS = (D/\pi)^{1/2}(\partial/\partial t)\int_0^t (C_p)_{x=0}(t-\tau)^{-1/2}\,d\tau. \tag{A4}$$

Equation (8) is obtained by the method of numerical integration of equation (A4). The increments of the product concentration $(C_p)_{x=0,k}$ are related to Θ_k through conditions (b), (d) and (e).